APPLICATION OF OIL-WATER KR/PC UPSCALING METHODOLOGY BASED ON PORE-TYPE RATIOS

Kazuhito Oseto, Osamu Himeno, Makoto Watanabe, Toshinori Nakashima
Japan Oil, Gas and Metals National Corporation (JOGMEC)

This paper was prepared for presentation at the International Symposium of the Society of Core Analysts held in Calgary, 10-12 September 2007

ABSTRACT

Our methodology provides fast and robust computation of upscaling by introducing a new averaging technique as a part of the capillary limit method, that is basically suited to giant, heterogeneous and oil wet reservoirs. In our past studies, its effectiveness was verified at core scale upscaling, i.e. pore scale to core scale, as well as reservoir simulation scale upscaling, i.e. fine model to coarse model. This paper introduces a practical approach for upscaling which bridges the various scales.

In this study, the reservoir rock from a giant carbonate reservoir in the Middle East was characterized as the aggregate of three Pore-Types. The representative Kr/Pc curves for each Pore-Type were derived from core flood simulation as a result of matching with water-oil displacement tests. Then, Pore-Type Ratio, i.e. the population ratio of each Pore-Type, was quantified by the geological observation of the core slabs for the whole interval of the reservoir. Based on the Pore Type Ratios, Kr/Pc curves were upscaled to the simulation grid scale using an in-house software called CAVLUP.

The simulation results showed that the Pore Type Ratio model reasonably reproduced water cut performances without any history matching manipulations. As a result, applied methodology in this study demonstrated its effectiveness to upscale pore scale data to reservoir simulation scale. This advantage is suited especially to the upscaling of big and heterogeneous geological models.

INTRODUCTION

For many of heterogeneous carbonate reservoirs, matching between production history of fluid flow behaviors and predicted performance by reservoir simulation is not straightforward. Although it is a key issue to obtain accurate Kr/Pc data, accurate laboratory measurements are not always secured with current technology for heterogeneous carbonate samples. Even if the laboratory measurements are reliable, plug data obtained through the laboratory measurement can only represent a localized property at the sampling point, which is not representing the simulation grid size. Hence, accurate

laboratory measurements, reliable upscaling techniques and appropriate techniques to combine them are required to be developed.

We developed a new averaging technique for absolute permeability upscaling [1] and incorporated it into the capillary limit method [2,3] and resultant in-house upscaling software called CAVLUP. This new technique leads to much less computation time for upscaling with accuracy provided that capillary force is dominant in the reservoir of interest.

Takahashi et al. [4] employed the CAVLUP to estimate core-scale Kro/Krw curves by upscaling pore-scale Kro/Krw curves. To extend it to reservoir simulation scale, in this study, (1) we first examined the reservoir cores to extract principal pore components (here we call them as 'Pore Types') representing the main reservoir interval. As a result, we defined three pore types for the main part of study reservoir and relative abundance of three Pore Types expressed the reservoir layers in the simulation model. (2) We generated representative Kr/Pc curves for each Pore Type by history matching of the coreflood experiments and core-scale simulation model. (3) Then we observed the cores covering the whole target interval, traced boundaries of different Pore Types at the core slab surface, and quantified the pore type ratios for the main reservoir layers of the simulation models.

In this paper, we introduce a practical way of obtaining reliable Kr/Pc curves for simulation grids scale by integrating the upscaling method of laboratory data and result of coreflood experiments. Using these newly obtained Kr/Pc curves, a new reservoir simulation model was built and prediction of production performance was compared with the original simulation model.

DEVELOPED UPSCALING TECHNIQUE

In all over the study, we applied in-house program called CAVLUP (CApillary and Viscous Limit UPscaling program) for upscaling. CAVLUP is based on effective properties approaches. The effective properties approaches take two advantages as compared to another existing method, i.e. dynamic approaches, since it calculates upscaled flow properties within each target coarse grid block. Firstly the effective properties approaches are case independent. In dynamic approaches, that are case dependent, different dynamicpseudos have to be generated for different flood rates and directions. Secondly, the effective properties approaches take less time for computation. The latter advantage is important especially in a big model. However further

improvement have been still required for a giant model that came up as increasing necessity of a detailed geological model to tackle with reservoir heterogeneity. We tried to improve this aspect by introducing new average method.

SINGLE PHASE UPSCALING

There are two major categories in the existing methods to calculate upscaled absolute permeability: algebraic techniques (e.g. harmonic, arithmetic, geometric, power averaging or a combination of harmonic and arithmetic methods) and pressure solver techniques (direct simulation methods). The former is fast but less accurate while the latter is accurate but very time consuming. We tried to improve the algebraic techniques by conducting intensive numerical experiments. As a result, we obtained the following new correlation;

$$\log(k_{ups\_h}) = 0.016 + 0.632\log(k_h^-) + 0.363\log(k_h^+) \quad (1)$$

$$\log(k_{ups\_v}) = 0.018 + 0.871\log(k_v^-) + 0.123\log(k_v^+) - 0.006(\log(k_v^+))^2 \quad (2)$$

where, k^+ and k^- are upper and lower bound permeability defined by Li. et. al respectively. Figure 1 shows upper and lower bound permeabilities and effective permeabilities upscaled by the developed correlation versus true effective permeabilities by a pressure solver. The developed equations provide high prediction quality.

TWO PHASE UPSCALING

Steady state upscaling [2,3] is a central part of the effective properties approaches. This technique determines saturation distribution within an upscaled domain assuming flow conditions such as viscous limit or capillary limit and calculates effective phase permeability using a single-phase steady state flow simulation. Hence, the above correlation can be utilized even in two phase properties upscaling, i.e. Kr and Pc upscaling.

Suzuki et. al [7] demonstrated that the developed technique made history matching for a multi-million detailed geological model significantly accelerated and practical.

Thus, CAVLUP and its new averaging method make upscaling for a big model more practical by reducing computation time.

UPSCALING OF Kr/Pc DATA OBTAINED IN LABORATORY

As mentioned earlier, in the past study, we applied the capillary limit method to upscaling from pore-scale to core-scale. Core samples taken from a heterogeneous carbonate reservoir in the Middle East were dedicated to the study. Water displacement tests and

following coreflood simulations were carried out on the 1 inch-diameter plug samples. The 3D coreflood models were constructed from available data such as X-ray CT porosity/ Swi/ Sor, minipermeameter permeability. We defined Pore-Type based on petrographical and petrophysical analysis such as core / thin section observation, SEM, mini-permeameter permeability, pore-throat size distribution and so on. The Pore Type of the studied cores was classified into three categories as will hereinafter be described in detail. The unknown parameters of kro/krw and Pc curves of each Pore-Type were derived from the matching with the experimental data such as changes of water saturation of each grid-cell derived from X-ray CT and differential pressure during the test.

Based on the data derived from the interpretation of the water displacement tests on the plug cores, a 3D base model was constructed for the whole core as well as hundreds of sister models were experimentally generated.

In the base model, firstly, the geologist assigned one of the three Pore-Types to each of the grid cells as well as corresponding Kr/Pc curves derived based on the experiments for the plug samples, secondary, Kr/Pc curves for each Pore Type were re-tuned to allow better matching with the water displacement test data for the whole core, and finally those curves were upscaled by CAVLUP.

In the sister models, the three Pore-Types and the three corresponding Kr/Pc curves were randomly distributed to grid-cells, while keeping population ratio constant among the models. The spatial distributions of porosity and permeability were varied as well within the range of the actual measurement data obtained from X-ray CT and minipermeameter. No correlation between two phase properties, i.e. Kr/Pc, and porosity/permeability was considered for the moment. We upscaled Kro/Krw curves for each of the sister models generated in this manner.

Figure 2 shows the plot where the upscaled kro/krw curves in hundreds of the sister models is overlaying. As seen in the figure, all the kro/krw curves almost converged into one curve. Figure 3 compares the Kro/Krw curves from the base model and that estimated by averaging a hundred curves of the sister models. It is shown that both curves reasonably agree each other. This means that upscaled kro/krw curves are not affected by the spatial distribution of the permeability and Pore Types and can be accurately obtained once the population ratios of Pore-Types are fixed, for example, by means of geological examination on its slab cores.

EXTENSION TO RESERVOIR SIMULATION SCALE

The above findings led to one practical approach for upscaling which bridges the gap between core-scale and reservoir simulation-scale. More specifically, once the population ratios of Pore-Types are generated by core observation for the whole interval of the reservoir of interest, we can obtain upscaled kro/krw curves for the whole interval of the reservoir incorporating pore scale characteristics. The procedure to verify this approach is summarized as follows;

i) Classification of Pore Types
ii) Generation of representative Kr/Pc curves for each pore type by coreflood experiments and simulation matching
iii) Generation of the distribution of Pore Type Ratios for the whole interval of the target reservoir
iv) Upscaling of the Kr/Pc curves to reservoir simulation grid scale using CAVLUP
v) Implementation of reservoir simulation

The reservoir of interest is a giant carbonate reservoir in the Middle East. Five-spot pattern water injection has been conducted for more than 20 years. The open hole logs and pulsed neutron logs conducted in the observation wells indicate that the injected water is preferentially advancing in relatively thin horizons. The water slumping appears to be prevented by the underlying horizons by capillary holding mechanism due to strong oil wetness and the heterogeneity [8]. Hence, the upscaling methodology mentioned above was expected to be applicable.

CLASSIFICATION OF PORE TYPES

Based on the detailed petrographical and petrophysical analysis, the sub-region pore-type composing the core was finally classified into three categories, i.e. Type A: Coarse-grain PKST/GRST, Type B: Fine-grain PKST/WKST and Type C: Algal fragment (or Algal grain). Type A corresponds to relatively well-sorted and coarse Lithocodium rudstones and packstones (grain size less than 5 mm) that make up the basal part of upward-fining units deposited under a strong influence by storm event (so-called storm beds). Type A also includes burrow-filling coarse materials surrounded by muddy packstones. Burrow-fills are usually observed below the storm beds. Type B is muddy packstones deposited during a fair weather background period. Type B occurs below and in-between the storm beds. Type C corresponds to a single algal grain differentiated from Type A based on grain size showing over 5mm. Figure 4 shows the summary of the classification of the Pore-Type.

GENERATION OF REPRESENTATIVE Kr/Pc CURVES FOR EACH PORE-TYPE BY COREFLOOD EXPERIMENTS AND SIMULATION MATCHING

Water displacement tests and following coreflood simulations were carried out on the three plug core samples in the same manner as previously described. The in-house coreflood simulation matching program called "GEMAP [9]" was employed for this interpretation. Figure 5 shows the example of the matching result of the water displacement test in terms of the average water saturation changes in the positions of every 5mm distance from the inlet. The degree of the matching of this test as well as the other two tests, though they were not shown in this paper, was quite acceptable from our experience. As a result, a unique set of kro/krw and Pc curves was derived for the three Pore-Types. (Figure 6 shows normalized curves)

GENERATION OF THE DISTRIBUTION OF PORE TYPE RATIOS FOR THE WHOLE INTERVAL OF THE TARGET RESERVOIR

A reference reservoir model was a sector model having 8km×8km in area, 215×215×73 fine grid cells, subsequently the area of each grid cell was 56m×56m. The formation thickness ranges from 140ft to 150ft. The sector contains 40 active wells (16 producers and 24 injectors). Our intention was to scale up to 54×54×36 coarse grid cells with 224m×224m in area for each grid cell.

Pore Type Ratio, that is defined as the population ratio of each Pore Type within the volume (or area) of interest, was required to be determined for each layer for the upscaling to reservoir simulation scale. The geologist intensively observed the core slabs of the well located at the centre of the sector for the whole interval of the producing reservoir and calculated the area ratio of each Pore Type. Figure 7 shows a typical example of the core observations. Pore Type Ratios for the whole interval are listed in Table 1. It was noticed that Pore Types other than the classified three pore types exist in some parts of the reservoir. Kr/Pc curves originally allocated in the existing model were basically used in this case.

UPSCALING OF THE Kr/Pc CURVES TO RESERVOIR SIMULATION GRID SCALE

Pore Type Ratios for the fine layers were averaged by layer thickness weighted arithmetic mean according to the coarse layer framework as shown in Table 2 as an example. Then, one realization of the spatial distribution of the three Pore Types was

arbitrarily generated based on the averaged Pore Type Ratios, and Kr/Pc curves were upscaled using CAVLUP.

Figure 8 shows the upscaled Kr/Pc curves for all the coarse layers. The upscaling was conducted on the normalized curve basis, therefore, actual grid Kr/Pc curves should be scaled by the end points i.e. Swc and Sor.

IMPLEMENTATION OF RESERVOIR SIMULATION

The upscaled Kr/Pc curves based on Pore Type Ratios were incorporated into the existing model replacing the original Kr/Pc. Figure 9 highlights the comparison of calculated water cut performances with actual water cut data for the wells located relatively in the centre of the sector. There was a difficulty in getting match with the actual water cut data in the existing model, which led to many local adjustments of the endpoints of Kr curves. However, as shown in Figure 9, the Pore Type Ratio model generally shows good matching to the actual water cut data. It should be highlighted that we obtained the good matching without any change in parameters other than introducing the new upscaled Kr/Pc curves based on the Pore Type Ratios. Figure 10 compares the calculated vertical Sw distributions between the Pore Type Ratio model and the existing model at the observation well which is located at the centre of the sector. The black dots on the figure correspond to interpreted Sw values from the time lapse pulsed neutron logs. It is seen that the Pore Type Ratio model reproduced vertical Sw distribution better than the existing model. Thus, our upscaling methodology demonstrated the capability of directly bridging between micro scale characterization and reservoir simulation model.

CONCLUSIONS

Upscaled Kr and Pc curves were generated for coarse block along the well based on the Pore Type Ratios by the core observation and incorporated into the sector model. The simulation results showed that the Pore Type Ratio model reasonably reproduced water cut performances without any history matching manipulations. As a result, the applied methodology demonstrated its effectiveness to upscale pore scale data to reservoir simulation scale in a consistent manner. It is to be highlighted the methodology is simple and practical in conjunction with fast and robust computation technique of upscaled permeabilities. This advantage is suited especially to the upscaling of big and heterogeneous geological models.

NOMENCLATURE

Kr=Relative permeabilities Pc=Capillary pressure

Kro= Oil phase relative permeability Krw=Water phase relative permeability

K_{ups_h}=Upscaled horizontal permeability

k_h-=Lower bound horizontal permeability defined by Li. et. al

k_h+=Upper bound horizontal permeability defined by Li. et. al

k_{ups_v}=Upscaled vertical permeability

k_v-=Lower bound vertical permeability defined by Li. et. al

k_v+=Upper bound vertical permeability defined by Li. et. al

Swi=Irreducible water saturation Sor=Residual oil saturation

Swc=Critical water saturation

ACKNOWLEDGEMENTS

This study was supported by Japan Oil Development Company, Ltd. The authors would also like to thank Abu-Dhabi National Oil Company for granting permission to publish this article.

REFERENCES

1. Nomura, M.: “Fast and Robust Computation of Effective Permeabilities” paper SPE 78517 prepared for presentation at the 10th Abu Dhabi International Petroleum Exhibition and Conference held in Abu Dhabi, UAE, 13-16 October 2002.
2. Pickup, G.E., and Sorbie, K.S.: “The scale-up of Two-Phase Flow in Porous Media Using Phase Permeability Tensors,” SPEJ, vol. 1, 369-381, Dec. 1996.
3. Pickup, G.E., Ringrose, P.S., and Ahmed Sharif: “Steady-State Upscaling: From Lamina-Scale to Full-Field Model,” SPEJ, vol. 5, 208-217, June 2000.
4. Takahashi, S., Tokuda, N., and Nakashima, T.: “Upscaling Method of Relative Permeability from Plug Core to Whole Core”, paper SCA 2004-16 presented at the Society of Core Analysts Symposium, 5-9 October, 2004 , Abu Dhabi, UAE.
5. Cardwell, W.T. JR., and Parsons, R.L.: “Average Permeability of Heterogeneous Oil Sands,” Trans. AIME, No.160, 34-42 1945.
6. Li, D., Beckner, B., and Kumar, A.: “A New Efficient Averaging Technique for Scale-up of Multimillion-Cell Geologic Models,” SPEFE, August 2001.
7. Suzuki, K., Asada, J., Yoshida, K., and Nomura, M.: :“Accelerated History Matching Through Process Independent Scale-up Techniques in a Giant Carbonate Reservoir”, paper SPE 87012, presented at the SPE Asia Pacific Conference on Integrated Modelling for Asset Management held in Kuala Lumpur, Malaysia, 29-30 March 2004.

8. Namba, T., and Hiraoka, T.: “Capillary Force Barriers in a Carbonate Reservoir Under Waterflooding,” paper SPE 29773 presented at the 1995 SPE Middle East Oil Show, Bahrain, Mar. 11-14.
9. Tokuda, N., Takahashi, S., Watanabe, M., and Kurose, T.: “Development of Automated History-matching Program Based on Genetic Algorithm for X-ray CT Coreflooding Experiment” paper SCA 2004-14 presented at the Society of Core Analysts Symposium, 5-9 October, 2004 , Abu Dhabi, UAE.

Table 1 Observed Pore Type Ratios

Layer #	Pore Type Ratio (%)			Layer #	Pore Type Ratio (%)			Layer #	Pore Type Ratio (%)		
	Type A	Type B	Type C		Type A	Type B	Type C		Type A	Type B	Type C
1*	0.00	0.00	0.00	26	44.94	52.42	2.64	50	3.58	96.09	0.34
2*	0.00	0.00	0.00	27	58.57	34.97	6.46	51	16.58	82.04	1.38
3*	7.96	18.66	1.10	28*	0.00	12.04	0.01	52	100.00	0.00	0.00
4*	0.00	0.00	0.00	29	35.47	61.82	2.71	53	99.42	0.00	0.58
5*	0.00	0.00	0.00	30	89.73	6.46	3.81	54	77.25	16.11	6.64
6*	37.84	0.00	0.00	31	28.48	69.47	2.05	55	69.65	29.49	0.85
7*	0.00	9.32	0.32	32	3.61	96.39	0.00	56	65.85	32.95	1.20
8*	0.00	0.00	0.00	33	2.94	96.00	1.06	57	13.47	85.27	1.25
9*	0.78	43.98	0.43	34	7.84	90.57	1.59	58	13.91	84.12	1.96
10	0.00	99.05	0.95	35	18.98	79.21	1.80	59	6.08	91.78	2.14
11	2.19	97.20	0.61	36	100.00	0.00	0.00	60	0.00	93.42	6.58
12	100.00	0.00	0.00	37	35.69	63.14	1.17	61*	1.82	29.37	0.50
13	8.31	91.15	0.54	38	11.50	86.94	1.56	62*	2.22	24.70	0.76
14	11.28	86.89	1.84	39	8.73	90.31	0.96	63*	6.47	23.03	1.01
15	10.39	88.13	1.48	40	1.56	96.76	1.68	64*	1.38	19.69	0.50
16	25.01	73.89	1.10	41	45.18	53.47	1.35	65*	44.69	6.37	0.57
17	13.43	85.59	0.97	42*	0.00	0.00	0.00	66*	2.86	31.96	0.09
18	99.09	0.00	0.91	43*	0.00	0.00	0.00	67*	0.00	37.78	0.67
19	12.90	86.42	0.68	44	86.99	5.62	7.38	68*	7.75	72.25	1.76
20	16.45	82.18	1.37	45	36.62	59.44	3.94	69*	5.70	90.83	1.34
21	4.63	94.87	0.50	46	80.54	16.87	2.60	70*	8.38	58.97	1.98
22	99.01	0.00	0.99	47	21.39	76.93	1.68	71*	9.96	18.23	0.83
23	8.08	89.52	2.40	48	81.62	16.80	1.58	72*	27.20	5.23	0.28
24	75.16	23.38	1.46	49	26.12	71.69	2.19	73*	6.64	28.12	0.82
25	3.71	95.92	0.37								

* Pore Types other than the classified three pore types exist partly or entirely

Table 2 Example of upscaled Pore Type Ratios by layer thickness weighted arithmetic mean

Layer # (Fine)	Pore Type Ratio (% : measured)			Up-layered #	Layer thickness	Up-layered Pore Type Ratioo (%)		
	Type A	Type B	Type C			Type A	Type B	Type C
30	89.73	6.46	3.81	**28**	6.51E-01	**48.92**	**48.45**	**2.64**
31	28.48	69.47	2.05		1.30E+00			
32	3.61	96.39	0.00	**27**	6.18E-01	**23.38**	**75.53**	**1.08**
33	2.94	96.00	1.06		1.23E+00			
34	7.84	90.57	1.59		6.66E-01			
35	18.98	79.21	1.80		1.33E+00			
36	100.00	0.00	0.00		8.45E-01			
37	35.69	63.14	1.17		1.69E+00			
38	11.50	86.94	1.56		7.74E-01			
39	8.73	90.31	0.96		1.55E+00			
40	1.56	96.76	1.68	**26**	9.37E-01	**30.64**	**67.90**	**1.46**
41	45.18	53.47	1.35		1.87E+00			

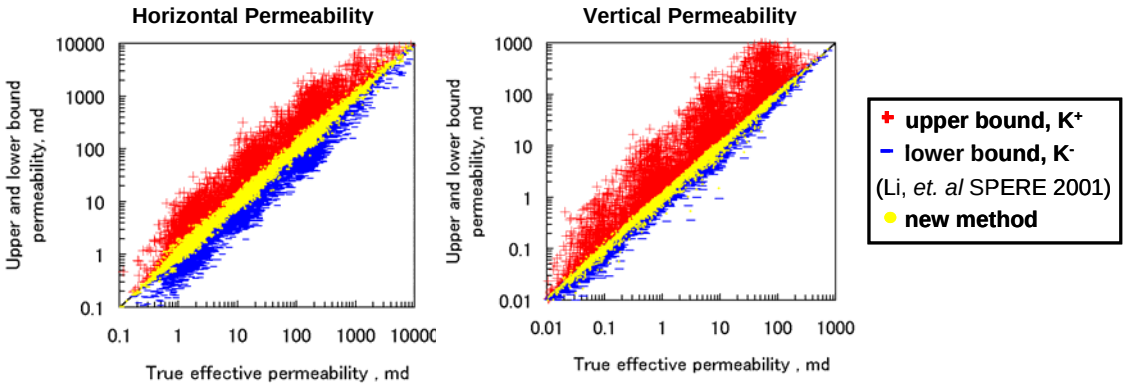

Figure 1 Effective permeabilities upscaled by the developed correlation versus true effective permeabilities by a pressure solver

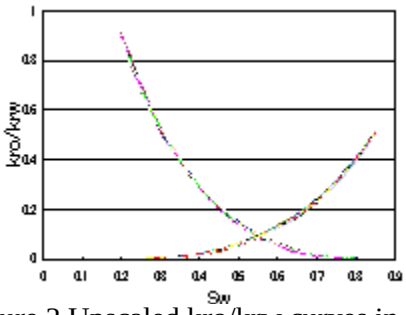

Figure 2 Upscaled kro/krw curves in the sister models

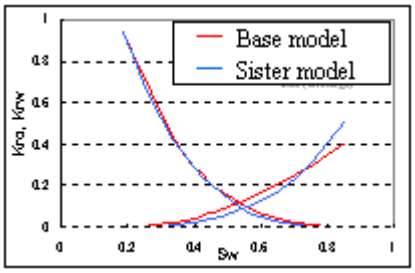

Figure 3 Comparison of the Kro/Krw curves from the base model and the sister

Pore-type (Properties)	**Photomicrograph**	**Air-permeability (md)**	**Porosity (%)**	**Pore Throat Size Distribution**
Pore-type A **Coarse PK/GRst** (Burrow fill Intergranular Pore, Micro Pore)	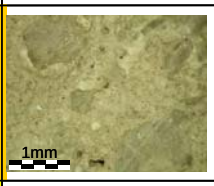	23 - 228	28 - 32	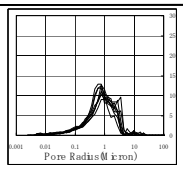
Pore-type B **Fine WK/PKst** (Micrite, Matrix Micro Pore)	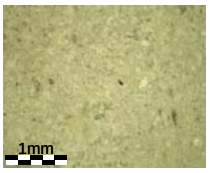	8 - 35	22 - 32	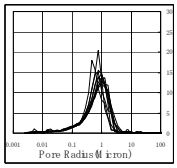
Pore-type C **Algal Fragment** (Intragranular Pore, Vug)		24 - 40	28 - 30	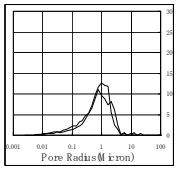

Figure 4 Summary of the classification of Pore-Type

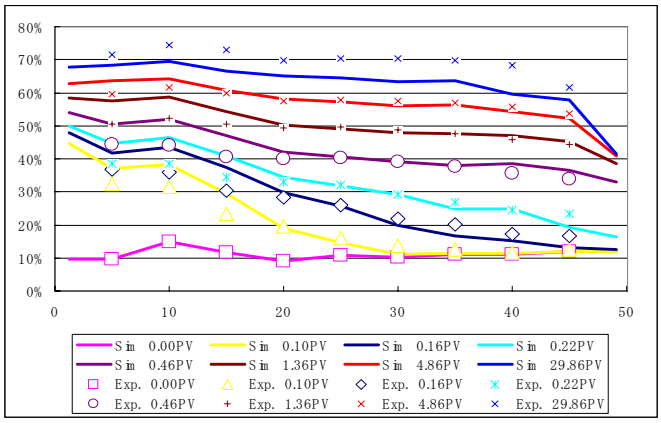

Figure 5 Example of the matching result of the water displacement test in terms of the average water saturation changes

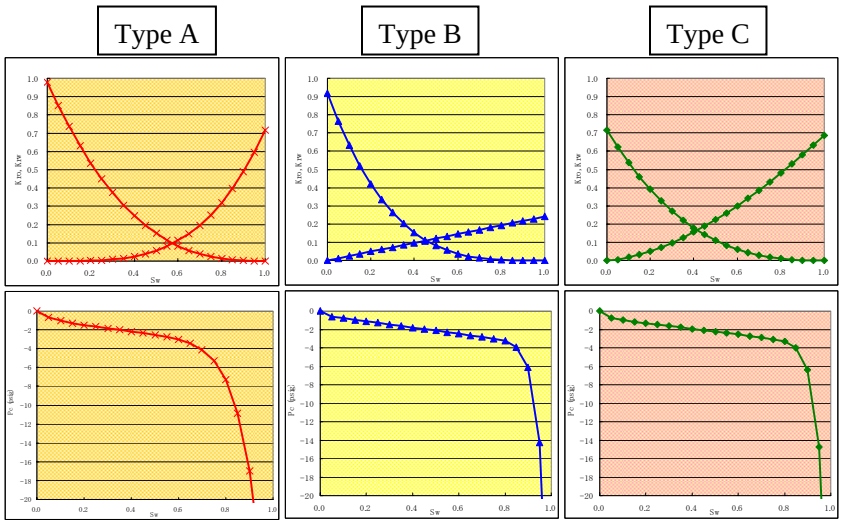

Figure 6 kro/krw and Pc curves was derived for each of the three Pore-Types

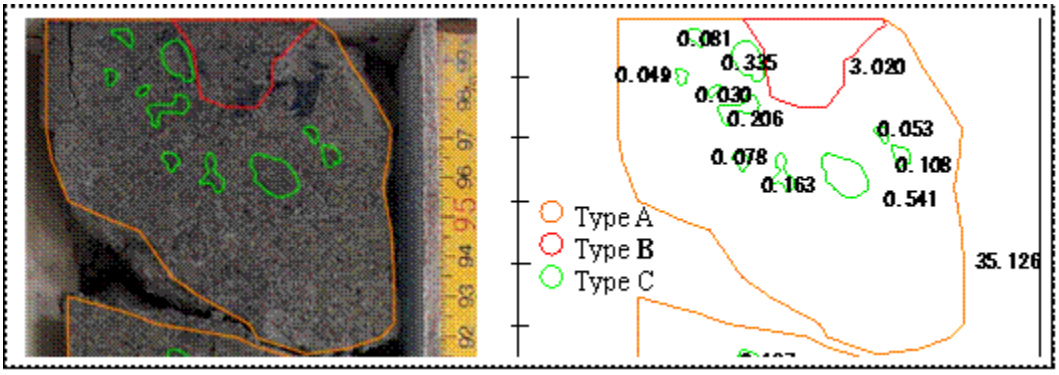

Figure 7 Typical example of core observations to calculate Pore Type Ratios

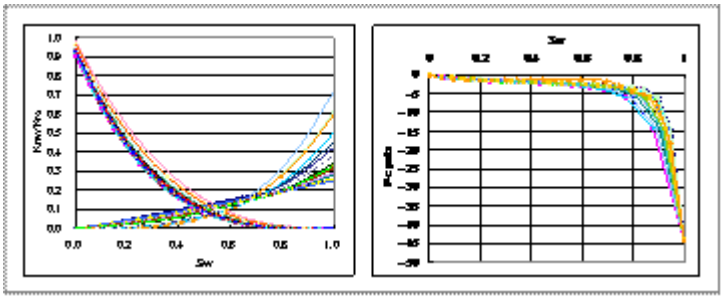

Figure 8 Upscaled Kr/Pc curves based on the Pore Type Ratios

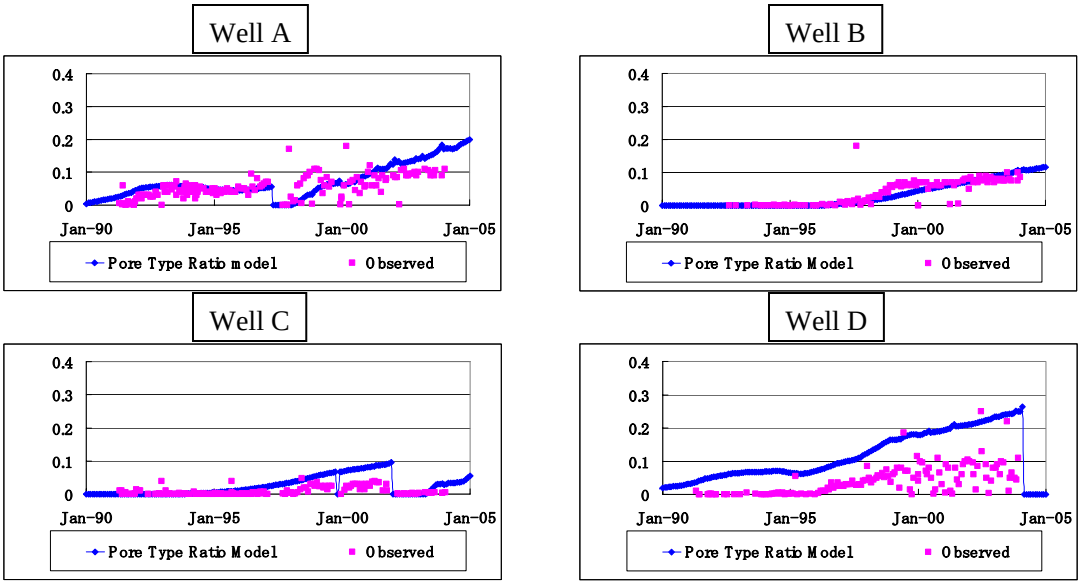

Figure 9 Upscaled Kr/Pc curves based on the Pore Type Ratios

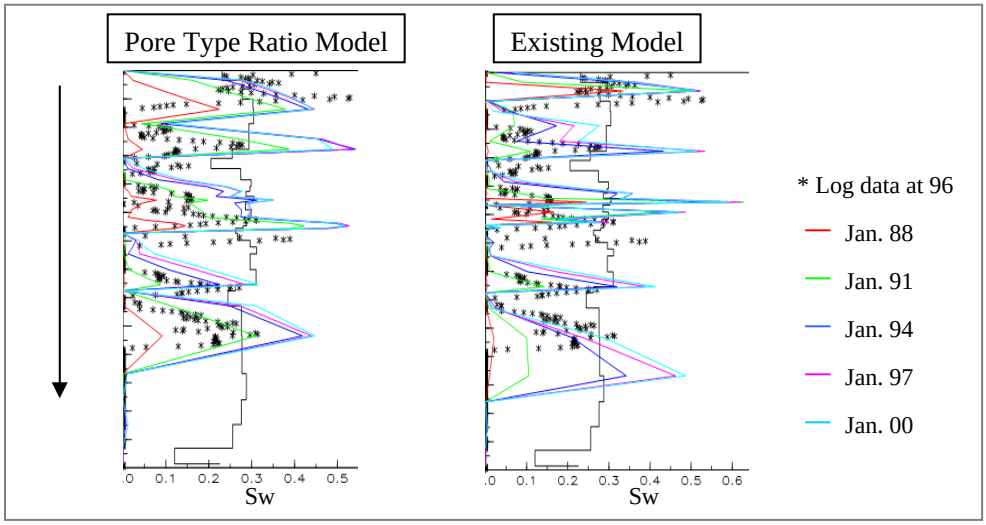

Figure 10 Comparison of the calculated vertical Sw distributions between the Pore Type Ratio model and the existing model